

BJP

Bangladesh Journal of Pharmacology

Research Article

Effects of shenkang injection on renal angiogenesis in mice with unilateral ureteral obstruction

Effects of shenkang injection on renal angiogenesis in mice with unilateral ureteral obstruction

Yajing Pan¹, Lu Zhang², Tonghua Liu¹ and Lili Wu¹

¹Key Laboratory of Health Cultivation of the Ministry of Education, Beijing University of Chinese Medicine, Beijing, 100029, China; ²School of Chinese Medicine, Shandong University of Traditional Chinese Medicine, Shandong, 250355, China.

Article Info

Received: 30 June 2019
Accepted: 13 February 2020
Available Online: 9 March 2020
DOI: 10.3329/bjp.v15i1.42052

Cite this article:

Pan Y, Zhang L, Liu T, Wu L. Effects of shenkang injection on renal angiogenesis in mice with unilateral ureteral obstruction. Bangladesh J Pharmacol. 2020; 15: 24-31.

Abstract

This study aimed to investigate effects of shenkang injection on angiogenesis in mice with renal fibrosis. C57BL/6J mice after unilateral ureteral obstruction were administrated with different doses of shenkang injection for two weeks. Losartan-administrated mice and Sham-operation mice were as positive and negative controls, respectively. Renal function and vasculature changes were observed, and expressions of VEGF and VEGFR₂ were detected. Shenkang injection reduced serum levels of urea nitrogen, creatinine and cystatin C. Shenkang injection alleviated the loss of microvessels, decreased the deposition of collagen fibers, and increased expressions of VEGF and VEGFR₂ in the obstructed kidney. These findings indicate that shenkang injection alleviates renal dysfunction and fibrotic changes in mice with renal fibrosis by regulating renal angiogenesis.

Introduction

Renal fibrosis is characterized by tubulointerstitial leukocyte infiltration, fibroblast proliferation, and increased matrix deposition. Renal fibrosis, consists of renal interstitial fibrosis and glomerular sclerosis, is a pathological hallmark of all chronic kidney diseases and results in end-stage renal disease. While current modern medicine is not effective in halting the progression of most chronic kidney disease, renal fibrosis is believed to represent an excellent treatment target of chronic kidney diseases (Stribos et al., 2016).

Shenkang injection is composed of radix et rhizoma rhei, radix astragali, radix et rhizoma salviae miltiorrhizae and flos carthami (Yao et al., 2014). Shenkang injection and its constituents are reported to minimize renal lesions by decreasing the levels of serum creatinine and blood urea nitrogen, suppressing oxidative stress and accumulation of extracellular matrix, and alleviating glomerular sclerosis and pathological lesions

in 5/6 nephrectomized rats (Liu et al., 2015; Wu et al., 2015; Liu et al., 2015; Zhang et al., 2014). Clinical studies have also suggested that combination of shenkang injection and alprostadil reduces the levels of urinary protein, serum creatinine, blood urea nitrogen, urinary albumin excretion rate and some serum inflammatory factors, and protects renal function in patients with chronic glomerulonephritis and chronic renal failure (Wang et al., 2016).

By means of a network research of pharmacological effects of shenkang injection on chronic kidney disease, vascular endothelial growth factor (VEGF) pathway is found to be involved in shenkang injection treatment for chronic kidney disease, and angiogenesis induced by VEGF may be a therapeutic target of shenkang injection treatment for chronic kidney disease. While little was known about the effects of shenkang injection on renal angiogenesis in previous studies, this study aimed to investigate potential protective effects of shenkang injection on renal angiogenesis.



Materials and Methods

Drugs and reagents

Shenkang injection was purchased from the Xi'an ShiJi ShengKang Pharmaceutical Industry Co., Ltd. (China) and losartan was purchased from the Merck Sharp & Dohme (China). Anti-vascular endothelial growth factor (VEGF; 19003-1-AP) and anti-vascular endothelial growth factor receptor 2 (VEGFR₂; 26415-1-AP) were purchased from the Proteintech Group, Inc. (USA).

Animals

Forty-eight specific pathogen-free male C57BL/6J mice, 8-week-old, weighing 20.8 ± 1.5 g, were supplied by the Beijing Vital River Laboratory Animal Technology Co., Ltd. (experimental animal license No. SCXK [Jing] 2016-0011). The mice were kept in a specific pathogen-free condition of (22 ± 3) centigrade and $(55 \pm 10)\%$ relative humidity under a 12/12 hours light/dark cycle, and freely provided with food and water.

Modeling and drug administration

The mice were randomly divided into six groups, each with the same body weight distribution (eight mice in each group): Sham group, unilateral ureteral obstruction group, losartan group, high-dose shenkang injection group (7.8 g/kg), moderate-dose shenkang injection group (3.9 g/kg), and low-dose shenkang injection group (1.95 g/kg). Mice were anesthetized with 1% pentobarbital sodium (80 mg/kg) via intraperitoneal injection. The left ureters were freed without ligation in Sham mice as negative controls. Mice except the sham ones were subjected to unilateral ureteral obstruction, in which the left ureters were ligated with silk thread at two ends and the parts between two ligatures were severed (Han et al., 2017). For the sham ones, the left ureters were freed without ligation.

Losartan was administrated by gavage at a dose of 13 mg/kg once daily in losartan group. Shenkang injection was administered via a tail vein once daily respectively. An equivalent amount of vehicle was administered to other groups via gavage administration or/and vein injection. The time and route of administration followed the instruction of shenkang injection and were in line with clinical use. And the dosage was converted from human dosage in clinic. Mice were sacrificed two weeks after administration (15 days after unilateral ureteral obstruction).

Measurement of blood urea nitrogen, creatinine and cystatin C

Blood were collected from the orbital venous plexus before sacrifice. Serum was separated by low-speed centrifugation (3,000 rpm at 4°C for 10 min). Levels of blood urea nitrogen, creatinine and cystatin C were determined by commercial assay kits. Operations

followed the manufacturers' protocols.

Micro-computed tomography

Renal vasculature was observed by micro-computed tomography according to the method described elsewhere (Ehling et al., 2016). Briefly, mice were anesthetized with 1% pentobarbital sodium (80 mg/kg) via intraperitoneal injection. For each mouse, after the thoracic cavity was opened, a blunt 22G needle was inserted into the cardiac apex and the auricula dextra was then severed. Vessels of systemic circulation were perfused with 30 mL of 0.9% saline, 30 mL of 4% paraformaldehyde, and 20 mL of microfil injection compounds (MV-122, Flow Tech, Inc., USA) via a perfusion pump (LSP04-1A, Baoding Longer Precision Pump Co., Ltd, China) successively. The entire carcasses were kept overnight at 4°C after clamping the cardiac apex and the auricula dextra. Kidneys were excised and fixed in 4% paraformaldehyde the next day. Kidneys were positioned on the rotation platform and scanned 360° around the vertical axis by a Siemens micro-CT scanner (Siemens Inveon Micro-CT, Germany). Images were acquired at 60 kV, 400 μ A. This resulted in 2048*2048 pixels images with resolution of 10.32 μ m. And 3D images were reconstructed by Siemens Inveon Research Workplace software 4.2.

Histology and immunohistochemistry

Kidneys were harvested immediately after sacrifice. Kidneys were fixed in 4% paraformaldehyde, embedded in paraffin, and cut into 4 μ m sections for histological evaluation. Parts of the sections were stained by hematoxylin and eosin to observe pathological changes, and by sirius red to observe fibrotic lesions and evaluate collagen deposition. Photographs of sections were taken by an Olympus microscope (BX53F, Olympus Co., Japan).

Other parts of the sections were used to perform immunohistochemical stains against VEGF and VEGFR₂. The extent of dyeing was observed, and average optical density of positive areas was calculated (average optical density = integral optical density/area).

Statistical analysis

The results of immunohistochemistry were carried out using ImageJ software (version 1.46; National Institutes of Health, USA). All quantitative data were analyzed by One-Way analysis of variance (ANOVA) using SPSS software (version 17.0; SPSS Inc., USA) and presented as mean \pm SD. P value <0.05 was considered as statistically significant.

Results

Effects of shenkang injection on blood urea nitrogen,

creatinine and cystatin C

As shown in Figure 1 (A, B, C), compared to sham mice, levels of blood urea nitrogen, creatinine and cystatin C increased significantly in unilateral ureteral obstruction mice ($p < 0.05$ or $p < 0.01$). And compared to unilateral ureteral obstruction mice, levels of blood urea nitrogen, creatinine and cystatin C decreased significantly in losartan and shenkang injection (7.8 g/kg) mice ($p < 0.05$ or $p < 0.01$).

Effects of shenkang injection on renal vasculature

As shown in Figure 2, compared to sham mice, unilateral ureteral obstruction mice had a dramatic reduction in numbers of blood vessels and vessel

branching, and a prominent decrease in vessel tortuosity in the left kidneys. Compared to unilateral ureteral obstruction mice, the number of blood vessels, vessel branching and vessel tortuosity increased, and the loss of microvessels alleviated in left kidneys of mice in losartan and shenkang injection (7.8, 3.9 and 1.95 g/kg) groups.

Effects of shenkang injection on renal pathology and fibrosis

As shown in tissue sections with hematoxylin and eosin stains (Figure 3), sham mice had normal renal structure with no obvious pathological damages and seldom inflammatory cells infiltration. Compared to sham mice, there were remarkable fibrotic changes with

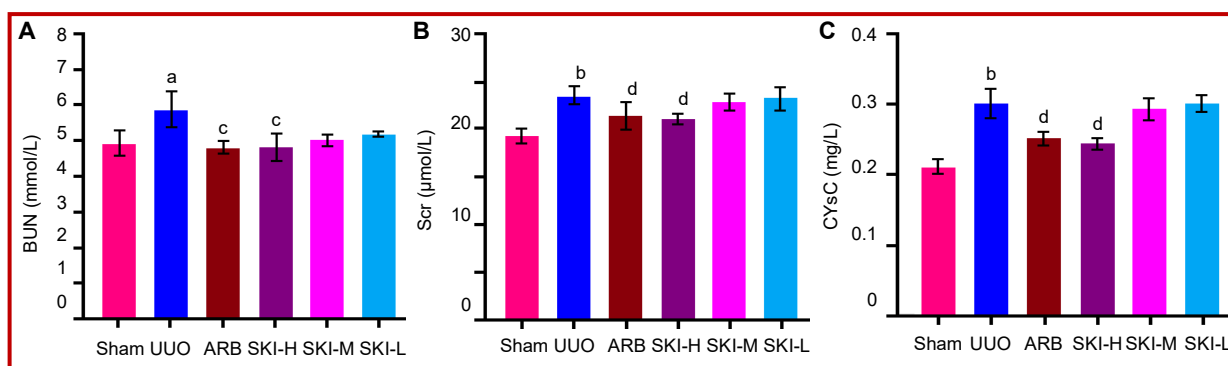


Figure 1: Effects of shenkang injection on blood urea nitrogen (BUN), serum creatinine (Scr) and cystatin C (CysC). The levels were determined by assay kits. Values are presented as mean \pm SD; ^a $p < 0.05$ vs sham group, ^b $p < 0.01$ vs sham group, ^c $p < 0.05$ vs UUO group, ^d $p < 0.01$ vs UUO group; ARB means losartan, UUO means unilateral ureteral obstruction; SKI-H means shenkang injection (7.8 g/kg); SKI-M means shenkang injection (3.9 g/kg); SKI-L means shenkang injection (1.95 g/kg)

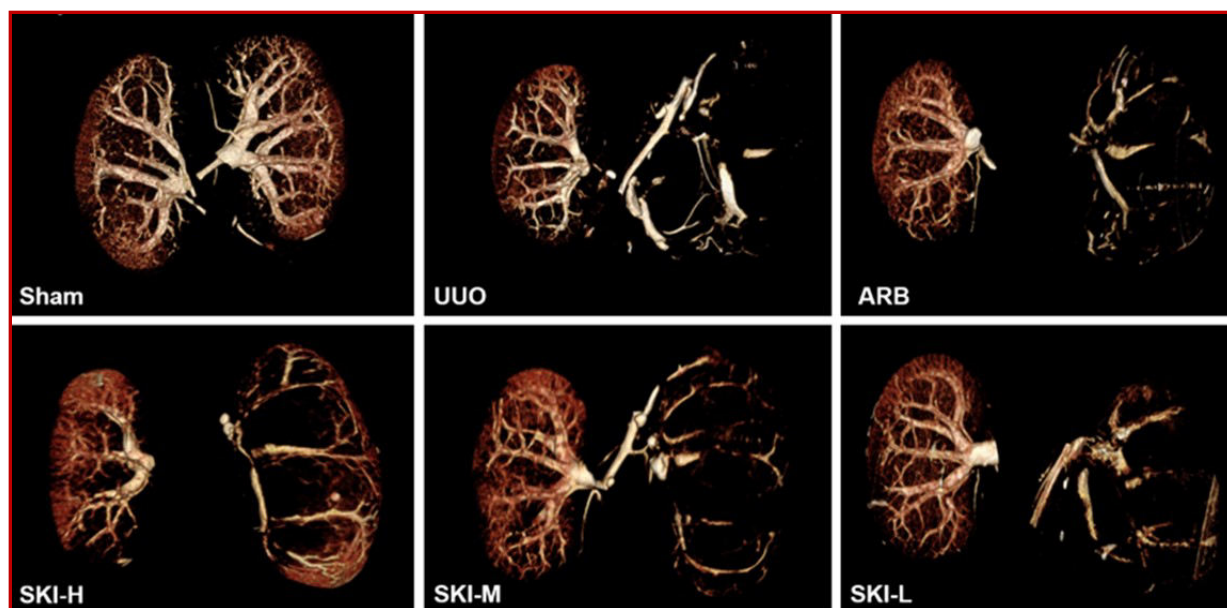


Figure 2: Effects of shenkang injection on renal vasculature. SKI-H means shenkang injection (7.8 g/kg); SKI-M means shenkang injection (3.9 g/kg); SKI-L means shenkang injection (1.95 g/kg); Renal vasculature was observed by micro-CT with a Siemens micro-CT scanner. 3D images were reconstructed by Siemens Inveon Research Workplace software 4.2

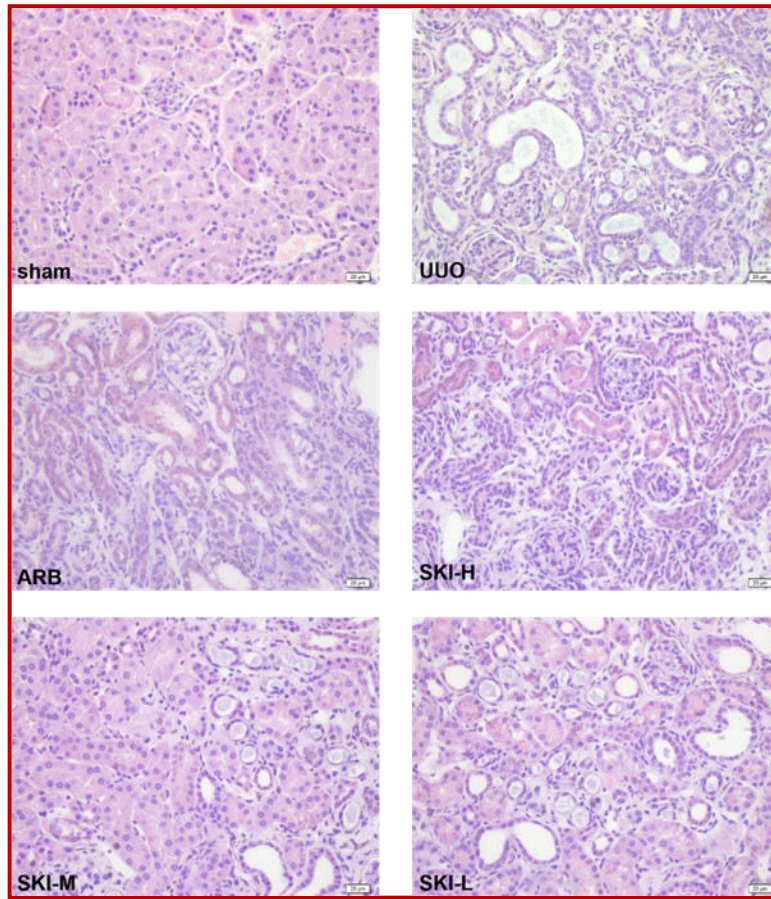


Figure 3: Effects of shenkang injection on renal pathology. Kidney biopsies were stained by hematoxylin and eosin to observe pathological changes (HE stains, 400 \times); SKI-H means shenkang injection (7.8 g/kg); SKI-M means shenkang injection (3.9 g/kg); SKI-L means shenkang injection (1.95 g/kg)

considerable tubular lumens dilatation, swollen renal tubular epithelial cells, enlarged renal interstitium and apparent inflammatory cells infiltration in unilateral ureteral obstruction mice. Compared to unilateral ureteral obstruction mice, fibrotic changes alleviated in mice of losartan and shenkang injection (7.8, 3.9 and 1.95 g/kg) groups.

As shown in tissue sections with sirius red stain (Figure 4A and 4B), seldom renal collagen fibers were observed in sham mice. Compared to sham mice, renal collagen fibers obviously increased in unilateral ureteral obstruction mice with sirius red stain showing red or orange birefringence under polarized light. And compared to unilateral ureteral obstruction mice, deposition of renal collagen fibers decreased in mice of losartan and shenkang injection (7.8, 3.9 and 1.95 g/kg) groups.

Effects of shenkang injection on VEGF and VEGFR₂

As shown by the extent of dyeing and average optical density of positive areas in Figure 5 (A, B), compared to sham mice, expression of VEGF decreased significantly in unilateral ureteral obstruction mice ($p < 0.01$). Com-

pared to unilateral ureteral obstruction mice, expression of VEGF increased significantly in mice of losartan and shenkang injection (7.8, 3.9 and 1.95 g/kg) groups ($p < 0.01$).

And as shown by the extent of dyeing and average optical density of positive areas in Figure 6 (A, B), compared to sham mice, expression of VEGFR₂ decreased significantly in unilateral ureteral obstruction mice ($p < 0.01$). Compared to unilateral ureteral obstruction mice, expression of VEGFR₂ increased significantly in mice of losartan and shenkang injection (7.8, 3.9 and 1.95 g/kg) groups.

Discussion

This study demonstrated that shenkang injection might be a therapeutic strategy for renal fibrosis by regulating renal angiogenesis. As far as we know, this is the first work that demonstrated effects of shenkang injection on renal fibrosis in mice with unilateral ureteral obstruction, targeting angiogenesis of renal vessels.

Previous studies have shown that shenkang injection

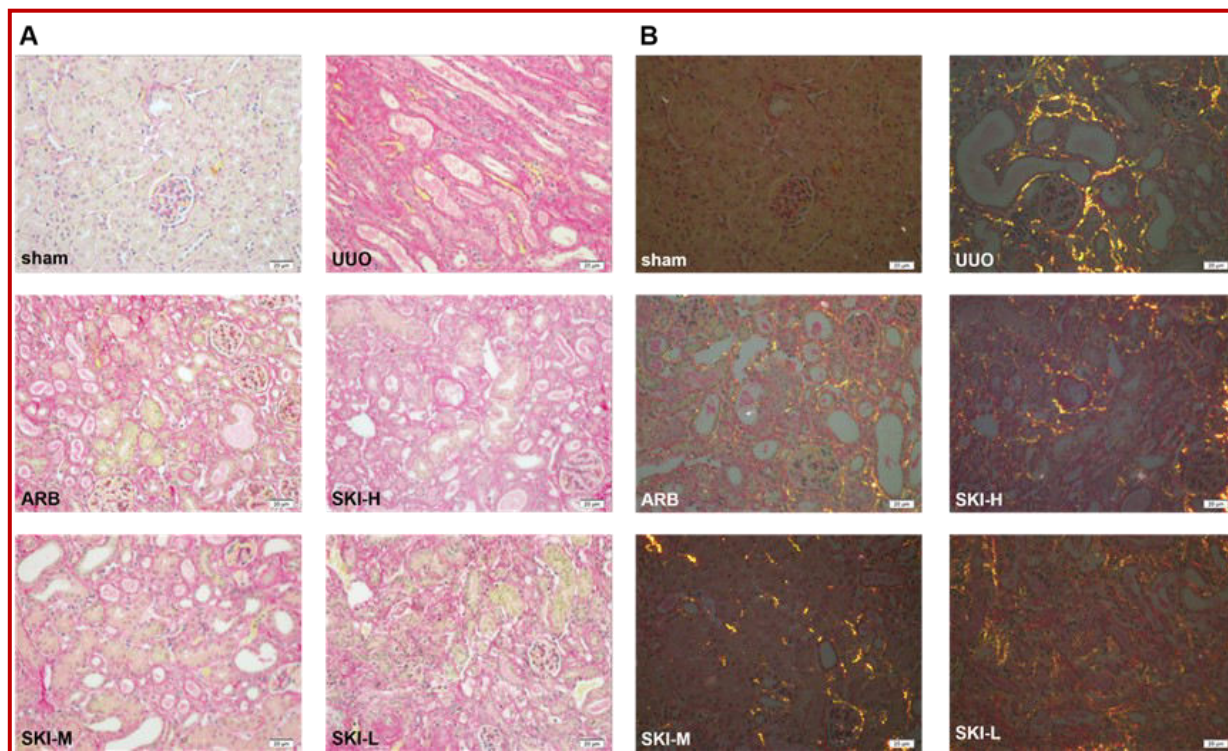


Figure 4: Effects of shenkang injection on renal fibrosis. Kidney biopsies were stained by sirius red stain to observe fibrotic lesions. (A) Sirius red stain, 400x, natural light; (B) Sirius red stain, 400x, polarized light; SKI-H means shenkang injection (7.8 g/kg); SKI-M means shenkang injection (3.9 g/kg); SKI-L means shenkang injection (1.95 g/kg)

could reduce serum levels of urea nitrogen, creatinine and cystatin C in 5/6 nephrectomized rats and streptozotocin-induced diabetic rats (Liu et al., 2015; Wu et al., 2015; Liu et al., 2015). In this study, shenkang injection was also found to decrease serum levels of urea nitrogen, creatinine and cystatin C significantly in mice with unilateral ureteral obstruction after administration via tail vein for 14 days ($p < 0.05$ or $p < 0.01$). Different from previous studies, unilateral ureteral obstruction model was used to investigate the effects of shenkang injection on renal fibrosis in this study. Unilateral ureteral obstruction is believed to mimic human chronic obstructive nephropathy and elucidate the pathogenesis of renal fibrosis, the common pathway in the progression of chronic kidney disease (Martinez et al., 2019; Chevalier et al., 2009). In obstructed kidney of unilateral ureteral obstruction, there are tubular dilation, interstitial expansion, loss of proximal tubular mass, hypertrophy, hydronephrosis, infiltration of inflammatory cells, tubular epithelial cell apoptosis and presence of fibroblasts, which altogether lead to progressive renal fibrosis (Martinez et al., 2019). These changes allow the use of experimental unilateral ureteral obstruction in rats and mice as a model to reproduce cardinal features of progressive chronic kidney disease in an accelerated fashion, and thus be used to address therapeutic approaches to kidney diseases (Ucero et al., 2014).

Typical pathological and morphological changes of renal fibrosis are tubular lumens dilatation, swollen renal tubular epithelial cells, enlarged renal interstitium and inflammatory infiltration (Chen et al., 2019). By hematoxylin and eosin stains, shenkang injection was found to alleviate these pathological and morphological changes in this study. And the most important fibrotic change is defined by formation and accumulation of extracellular matrix by kidney resident mesenchymal cells (Djudjaj et al., 2019). By sirius red stain, shenkang injection was found to decrease the deposition of collagen fibers, the basic components of extracellular matrix in this study. Altogether, shenkang injection was indicated to inhibit renal fibrosis by alleviating pathological changes and decreasing deposition of collagen fibers.

Studies have shown that renal fibrosis is paralleled by loss of micro-vessels, such as peritubular capillary rarefaction, and claimed that angiogenesis could be augmented as a therapeutic strategy for renal fibrosis in chronic kidney diseases (Humphreys, 2018; Majo et al., 2019). Here, micro-CT was used to visualize renal vessels. Micro-CT is highly reproducible and is believed to be a reliable approach in preclinical and basic kidney researches, especially useful in vasculature-related kidney pathologies such as renal fibrosis (Hlushchuk et al., 2018). In this study, it was obviously observed that unilateral ureteral obstruction mice had dramatic loss of

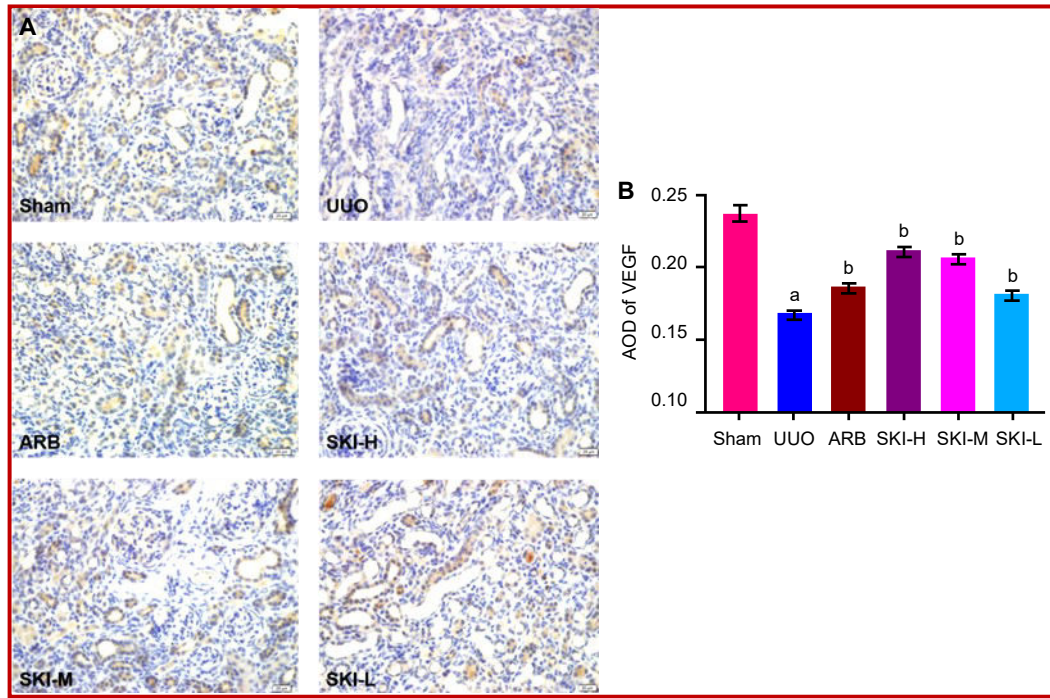


Figure 5: Effects of shenkang injection on expression of VEGF. (A) Expression of VEGF were determined by immunohistochemistry, 400×; (B) Average optical density (AOD) of positive areas was calculated. Values are presented as mean ± SD. ^ap<0.01 vs sham group, ^bp<0.01 vs UUO group; ARB means losartan; SKI-H means shenkang injection (7.8 g/kg); SKI-M means shenkang injection (3.9 g/kg); SKI-L means shenkang injection (1.95 g/kg)

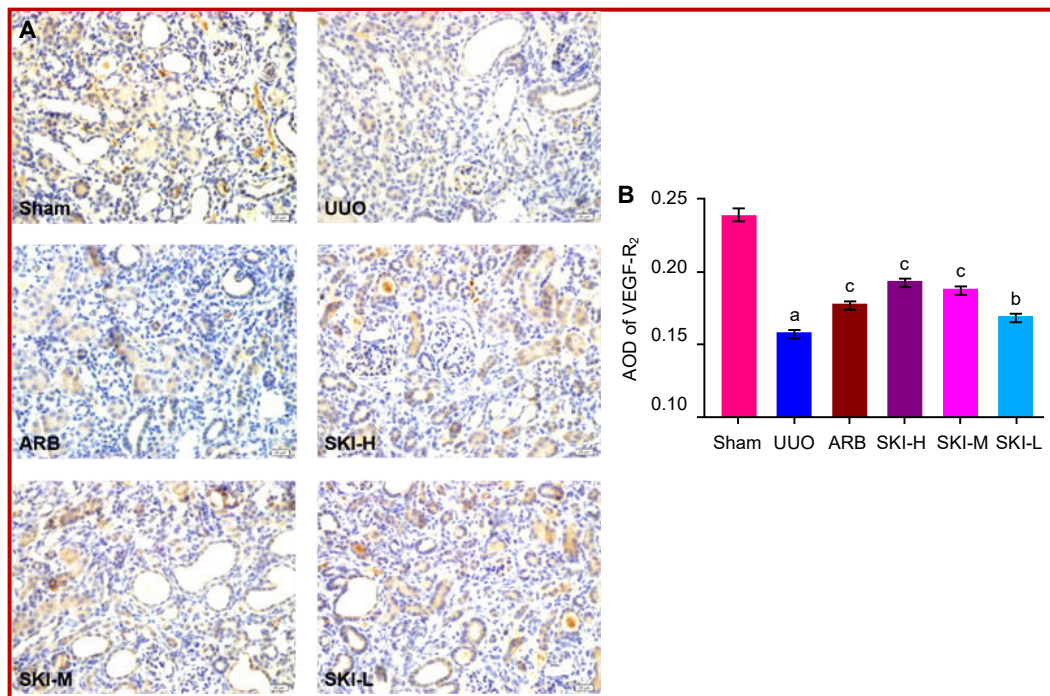


Figure 6: Effects of shenkang injection on expression of VEGFR₂. (A) Expression of VEGFR2 were determined by immunohistochemistry, 400×; (B) Average optical density (AOD) of positive areas was calculated. Values are presented as mean ± SD. ^ap<0.01 vs sham group, ^bp<0.05 vs UUO group, ^cp<0.01 vs UUO group; ARB means losartan; SKI-H means shenkang injection (7.8 g/kg); SKI-M means shenkang injection (3.9 g/kg); SKI-L means shenkang injection (1.95 g/kg)

microvessels in fibrotic kidneys compared with the sham mice by micro-CT, showing reduction in numbers of blood vessels and vessel branching, and decrease in vessel tortuosity in the left kidneys, which were in line with Ehling et al., 2016 and Lin et al., 2017. And shenkang injection alleviated loss of micro-vessels, showing obvious increases in numbers of blood vessels, vessel branching, and vessel tortuosity. As far as we know, this is the first work to demonstrate effects of shenkang injection on renal microvessels in mice with unilateral ureteral obstruction by micro-CT.

VEGF, the only specific mitogen to promote vasculogenesis and angiogenesis, plays an important role in modulating microvascular loss in the kidney (Chade et al., 2012). Recent studies have suggested that VEGF and VEGF-eNOS axis bioavailability decreased progressively in stenotic kidneys. Administration of VEGF can induce renal angiogenesis and alleviate renal fibrosis, and therefore VEGF therapy could provide a novel clinical approach in the treatment of chronic kidney disease (He et al., 2013; Stolz et al., 2015). By immunohistochemistry, expressions of VEGF and VEGFR₂ were found to decrease in obstructed kidney of unilateral ureteral obstruction mice, and shenkang injection was found to increase expressions of VEGF/VEGFR₂ in this study. Altogether, shenkang injection was indicated to regulate renal angiogenesis by alleviating loss of micro-vessels and increasing expressions of VEGF/VEGFR₂, and therefore might be a therapeutic strategy for renal fibrosis.

Conclusion

Shenkang injection alleviated renal dysfunction in mice with unilateral ureteral obstruction by decreasing blood urea nitrogen, creatinine and cystatin C, and inhibited renal fibrosis by alleviating pathological changes and decreasing deposition of collagen fibers. These effects might be related to regulating renal angiogenesis by alleviating loss of microvessels and increasing expressions of VEGF/VEGFR₂.

Ethical Issue

All experimental procedures were approved by the Ethics Committee for Animal Experimentation of Beijing University of Chinese Medicine.

Conflict of Interest

All authors declare that they have no conflict of interests.

Acknowledgements

Key Laboratory of Health Cultivation of the Ministry of

Education and Beijing University of Chinese Medicine are acknowledged. This study is supported by the Development of Science and Technology Project of Beijing University of Chinese Medicine: The mechanisms of effects of ShenKang Injection on chronic kidney disease (No. 2019-ZXFZJJ-001).

References

- Chade AR, Kelsen S. Reversal of renal dysfunction by targeted administration of VEGF into the stenotic kidney: A novel potential therapeutic approach. *Am J Physiol Renal Physiol.* 2012; 302: 1342-50.
- Chen PS, Li YP, Ni HF. Morphology and evaluation of renal fibrosis. *Adv Exp Med Biol.* 2019; 1165: 17-36.
- Chevalier RL, Forbes MS, Thornhill BA. Ureteral obstruction as a model of renal interstitial fibrosis and obstructive nephropathy. *Kidney Int.* 2009; 75: 1145-52.
- Djudjaj S, Boor P. Cellular and molecular mechanisms of kidney fibrosis. *Mol Aspects Med.* 2019; 65: 16-36.
- Ehling J, Babickova J, Gremse F, Klinkhammer BM, Baetke S, Knuechel R, Kiessling F, Floege J, Lammers T, Boor P. Quantitative micro-computed tomography imaging of vascular dysfunction in progressive kidney diseases. *J Am Soc Nephrol.* 2016; 27: 520-32.
- Han H, Zhu JZ, Wang YQ, Zhu ZB, Chen YJ, Lu L, Jin W, Yan XX, Zhang RY. Renal recruitment of B lymphocytes exacerbates tubulointerstitial fibrosis by promoting monocyte mobilisation and infiltration after unilateral ureteral obstruction. *J Pathol.* 2017; 241: 80-90.
- He JH, Xu Y, Koya D, Kanasaki K. Role of the endothelial-to-mesenchymal transition in renal fibrosis of chronic kidney disease. *Clin Exp Nephrol.* 2013; 17: 488-97.
- Hlushchuk R, Zubler C, Barré S, Correa Shokiche C, Schaad L, Röthlisberger R, Wnuk M, Daniel C, Khoma O, Tschanz SA, Reyes M, Djonov V. Cutting-edge micro-CT: New dimensions in vascular imaging and kidney morphometry. *Am J Physiol Renal Physiol.* 2018; 314: F493-99.
- Humphreys BD. Mechanisms of renal fibrosis. *Annu Rev Physiol.* 2018; 80: 309-26.
- Kohan D E, Barton M. Endothelin and endothelin antagonists in chronic kidney disease. *Kidney Int.* 2014; 86: 896-904.
- Lin YC, Hwu Y, Huang GS, Hsiao M, Lee TT, Yang SM, Lee TK, Chen NY, Yang SS, Chen A, Ka SM. Differential synchrotron X-ray imaging markers based on the renal microvasculature for tubulointerstitial lesions and glomerulopathy. *Sci Rep.* 2017; 7: 3488-99.
- Liu MY, Park J, Wu XX, Li YW, Tran Q, Mun K, Lee YJ, HUR GM, Wen AD, Park J. Shen-Kang protects 5/6 nephrectomized rats against renal injury by reducing oxidative stress through the MAPK signaling pathways. *Int J Mol Med.* 2015; 36: 975-84.
- Liu Y, Ma Q, Yang G, Zhao JH, Liu S, Ao QG, Du J, Wang XH, Cheng QL. Early renal tubulointerstitial changes and their interventions with shenkang injection in diabetic rats. *Nat Med J China.* 2015; 95: 289-93.
- Majo J, Klinkhammer BM, Boor P, Tiniakos D. Pathology and

- natural history of organ fibrosis. *Curr Opin Pharmacol*. 2019; 49: 82-89.
- Markwardt D, Holdt L, Steib C, Benesic A, Bendtsen F, Bernardi M, Moreau R, Teupser D, Wendon J, Nevens F, Trebicka J, Garcia E, Pavesi M, Arroyo V, Gerbes A. Plasma cystatin C is a predictor of renal dysfunction, acute-on-chronic liver failure, and mortality in patients with acutely decompensated liver cirrhosis. *Hepatology* 2017; 66: 1232-41.
- Martinez-Klimova E, Aparicio-Trejo OE, Tapia E, Pedraza-Chaverri J. Unilateral ureteral obstruction as a model to investigate fibrosis-attenuating treatments. *Biomolecules* 2019; 9: E141.
- Panetta D, Pelosi G, Viglione F, Kusmic C, Terreni M, Belcari N, Guerra AD, Athanasiou L, Exarchos T, Fotiadis DI, Filipovic N, Trivella M G, Salvadori P, Parodi O. Quantitative micro-CT based coronary artery profiling using interactive local thresholding and cylindrical coordinates. *Technol Health Care*. 2015; 23: 557-70.
- Stolz D B, Sims-Lucas S. Unwrapping the origins and roles of the renal endothelium. *Pediatr Nephrol*. 2015; 30: 865-72.
- Stribos E G, Luangmonkong T, Leliveld AM, Jong ID, Van Son W, Hillebrands J, Seelen MA, Van Goor H, Olinga P, Mutsaers HM. Precision-cut human kidney slices as a model to elucidate the process of renal fibrosis. *Transl Res*. 2016; 170: 8-16
- Ucero AC, Benito-Martin A, Izquierdo MC, Sanchez-Niño MD, Sanz AB, Ramos AM, Berzal S, Ruiz-Ortega M, Egido J, Ortiz A. Unilateral ureteral obstruction: Beyond obstruction. *Int Urol Nephrol*. 2014; 46: 765-66.
- Wang C, Gu ZF, Wang S, Shen LL, Zhang F. Effect of alprostadil combined with shenkang injection on urine protein, renal function and serum inflammatory in patients with chronic nephritis. *J Hainan Med*. 2016; 22: 2276-79.
- Wu XX, Guan Y, Yan JJ, Liu MY, Yin Y, Duan JL, Wei G, Hu TX, Weng Y, Xi MM, Wen AD. ShenKang injection suppresses kidney fibrosis and oxidative stress via transforming growth factor-beta/Smad3 signalling pathway *in vivo* and *in vitro*. *J Pharm Pharmacol*. 2015; 67: 1054-65.
- Xu TY, Zuo LH, Sun Z, Wang PL, Zhou L, Lv XJ, Jia QQ, Liu X, Jiang XF, Zhu ZG, Kang J, Zhang XJ. Chemical profiling and quantification of shenkang injection, a systematic quality control strategy using ultra high performance liquid chromatography with Q exactive hybrid quadrupole orbitrap high-resolution accurate mass spectrometry. *J Sep Sci*. 2017; 40: 4872-79.
- Yang J, Sun Z, Li DL, Duan F, Li ZL, Lu JL, Shi YY, Xu TY, Zhang XJ. A novel liquid chromatography orbitrap mass spectrometry method with full scan for simultaneous determination of multiple bioactive constituents of shenkang injection in rat tissues: Application to tissue distribution and pharmacokinetic studies. *Biomed Chromatogr*. 2018; e4306.
- Yao S, Zhang JX, Wang DD, Hou JJ, Yang WZ, Da J, Cai LY, Yang M, Jiang BH, Liu X, Guo DA, Wu WY. Discriminatory ingredients retracing strategy for monitoring the preparation procedure of Chinese patent medicines by integrating chemical fingerprint and chemometric analysis. *Plos One*. 2014; 6: 710-11.
- Zhang LX, Wang F, Wang L, Wang WK, Liu BC, Liu J, Chen MH, He Q, Yao YH, Yu XQ, Chen N, Zhang JE, Hu Z, Liu FY, Hong DQ, Ma LJ, Liu H, Zhou XL, Chen JH, Pan L, Chen W, Wang WM, Li XM, Wang HY. Prevalence of chronic kidney disease in China: A cross-sectional survey. *Lancet* 2012; 379: 815-22.
- Zhang Y, Zhou N, Li T, Wang HY, He JY. Effect of shenkang injection on kidney function in hypertensive renal damage rats. *Zhong Yao Cai*. 2014; 37: 2248-54.
- Zhang Y, Zhou N, Wang HY, Wang SC, He JY. Effect of shenkang granules on the progression of chronic renal failure in 5/6 nephrectomized rats. *Exp Ther Med*. 2015; 9: 2034-42.

Author Info

Lili Wu and Tonghua Liu (Principal contact)
e-mail: thliu@vip.163.com; qingniao_566@163.com